

# Block Adjustment-Based Radiometric Normalization by Considering Global and Local Differences

Xiaoshuang Zhang<sup>1</sup>, Ruitao Feng, Associate Member, IEEE, Xinghua Li<sup>2</sup>, Member, IEEE, Huanfeng Shen<sup>3</sup>, Senior Member, IEEE, and Zhaoxiang Yuan

**Abstract**—For radiometric normalization (RN) of multiple remote sensing (MRS) images within large-scale coverage, the traditional methods ignore the error accumulation and adaptive allocation of cumulative errors caused by the transfer paths in the classical one-after-another pipeline. To this end, a block adjustment-based RN method of MRS images is proposed by considering the global and local radiometric differences (RDs) in this letter. First, the block adjustment-based global RN is conducted to eliminate the global differences of MRS images. This step is independent of transfer paths so that it breaks through the corresponding error accumulation and uneven distribution in the one-after-another pipeline. Second, two local strategies based on block adjustment and edge optimization are further adopted to remove the local residual RDs. In the experiments, it demonstrates that the proposed method can obtain MRS images with a balanced and appealing visual effect, which outperforms the moment matching (MM) method and the popular ENVI software.

**Index Terms**—Block adjustment, local difference, moment matching (MM), radiometric normalization (RN), remote sensing image.

## I. INTRODUCTION

WITH the successful launch of remote sensing platforms, such as GeoEye series, WorldView series, and Planet, high-resolution images have become more and more widely used. However, high-resolution images have a limited range of coverage; thus, the acquisition of large-area images can only be achieved by mosaicking multiple remote sensing (MRS) images. Remote sensing images are usually acquired at different times and different angles, resulting in obvious radiometric differences (RDs) [1]. The influence factor mainly includes the solar incident angle, atmosphere, illumination condition, and so on [2]. Fortunately, radiometric normalization (RN) is an effective approach to eliminate the RDs among MRS

images. In a narrow sense, RN is the radiometric adjustment between multiple images, in order to solve the problem of significant difference in terms of radiation of multiple images. In the literature, RN is also called radiometric balancing, tonal adjustment, or tonal correction [3].

In the last decades, a great number of researches on RN of MRS images have been conducted [4]–[6], which can be classified into three categories [3]: global models, local models, and combined models. Global models represent the radiometric mapping relationship between the source and target images by a global linear or nonlinear transform, which are applicable to images with the overall consistent RDs. Global models can be further grouped into pixel-to-pixel methods and region-to-region methods. Pixel-to-pixel methods perform well for images with overall consistent RDs and high registration accuracy. Linear regression [7] and least mean square-based transformation [8] are the typical methods. Region-to-region methods are suitable for images with overall consistent RDs but do not require high accuracy of image registration. For instance, Sun *et al.* [9] eliminated RDs between images by the Wallis transform. Xie *et al.* [10] proposed a guided initial solution of the histogram extreme-point matching strategy for global consistency optimization to eliminate RDs. Xia *et al.* [11] proposed a closed-form solution for multiview color correction with gradient preservation. Li *et al.* [12] proposed a grid model-based global color correction method. Global models ignore the local RDs to some extent, but local models can solve this problem according to the regional features. For example, Li *et al.* [1] proposed a local moment matching (MM) method, which established different MM models in different regions. Li *et al.* [13] coarsely aligned the color tone between reference images and images to be corrected and removed RDs by least-squares RN. The combined models integrate the advantages of global and local models. For example, Pan *et al.* [14] proposed a global-to-local network-based RN to eliminate the RDs, in which the linear model is used globally and the nonlinear model is adopted locally. Yu *et al.* [2] proposed a global-to-local adaptive RN method, which can correct multiple types of remote sensing images with flexible process flow.

In a word, the traditional methods ignore the cumulative error and adaptive allocation of cumulative errors caused by transfer paths in the correction process. To solve this problem, this letter proposes an RN method of MRS images based on block adjustment considering local RDs (BARN). The main contributions of our study are summarized as follows.

Manuscript received June 18, 2020; revised August 20, 2020; accepted October 12, 2020. Date of publication October 28, 2020; date of current version January 4, 2022. This work was supported by the National Natural Science Foundation of China under Grant 41701394 and Grant 41971303. (Corresponding author: Xinghua Li.)

Xiaoshuang Zhang, Ruitao Feng, and Huanfeng Shen are with the School of Resource and Environmental Sciences, Wuhan University, Wuhan 430079, China (e-mail: zhangxiaoshuang@whu.edu.cn; ruitaofeng@whu.edu.cn; shenhf@whu.edu.cn).

Xinghua Li is with the School of Remote Sensing and Information Engineering, Wuhan University, Wuhan 430079, China (e-mail: lixinghua5540@whu.edu.cn).

Zhaoxiang Yuan is with the State Power Economic and Technological Research Institute Co. Ltd., Beijing 100120, China (e-mail: yuanzhaoxiang@chinasperi.sgcc.com.cn).

Digital Object Identifier 10.1109/LGRS.2020.3031398

- 1) Inspired by the block adjustment of bundle aerial triangulation, the proposed method simultaneously takes all images into account to calculate the correction parameters of RDs. The calculation is free from the influence of the processing order of MRS images. In other words, it is independent of the transfer paths with the inexistence of cumulative error.
- 2) The proposed method employs combined strategies to eliminate the RDs of MRS images globally and locally. After the global RDs are eliminated, the local residual RDs are further corrected by two local approaches. In the framework, the satisfactory result of an RN is achieved.

The rest of this letter is organized as follows. In Section II, the proposed method is introduced. The experiments are shown in Section III, followed by the conclusions in Section IV.

## II. METHOD

Based on the bundle aerial triangulation of block adjustment, this letter proposes to eliminate the RDs from global to local. As shown in Fig. 1, first, the block-adjustment-based RN eliminates the global RDs and alleviates the error accumulation and adaptive allocation of cumulative errors caused by transfer paths; second, two local strategies eliminate the residual discontinuity of the local features and edge artifacts.

### A. Block-Adjustment-Based Global RN

Selecting the reference image is an important step in most RN methods. The basic idea is to search the representative image with the global radiometric characteristics shared by the majority of images to be corrected. In order to estimate the tones globally, the mean image brightness is applied, which can reflect the visualization of an image. All images are converted from RGB color space to HSL color space, and the brightness layer of each image is extracted from the HSL color space. Then, the images corresponding to the mode of the mean brightness can be selected as the reference images.

In order to eliminate the global RDs and alleviate the error accumulation and adaptive allocation of cumulative errors caused by transfer paths, the global RN is adopted. This method mainly includes three steps: information statistics of overlapped region, block adjustment modeling, and MM correction.

*Step 1 (Information Statistics of Overlapped Area):* In the data set, there are  $p$  images and  $q$  overlapping pairs. Count the number of corresponding pixels in the overlapped region, and calculate the pixel mean and standard deviation of each band.

*Step 2 (Block Adjustment Modeling):* In this step, all the images are taken into account to model the block adjustment. We use the known conditions of the overlapped areas of adjacent images and the reference image to construct an error equation set, employ weights to scientifically evaluate the role of each overlapped area, and solve the tone compensation parameters in the block adjustment model with the help of least squares. This step is divided into five steps.

*Step 2.1:* Construct the matrix equation set by overlapped regions.

Assuming that the adjacent images have the same radiometric tone in the overlapped area, the statistics information of the radiometric tone should be the same. Taking the  $r$ th overlapped region as an example, it is formed by overlapping the adjacent  $x$ th image and  $y$ th image, which could be described in the following equation:

$$\mu_r^0 + \mu_x = \mu_r^1 + \mu_y \quad (1)$$

where  $\mu_r^0$  and  $\mu_r^1$  represent the pixel mean of the  $x$ th and  $y$ th images in the  $r$ th overlapped pair, respectively,  $\mu_x$  and  $\mu_y$  represent the unique pixel mean compensation parameters of the  $x$ th and  $y$ th images, respectively. Equation (1) can be written as

$$(b_{r,0} \ b_{r,1} \ \dots \ b_{r,p-1})(\mu_0 \ \mu_1 \ \dots \ \mu_{p-1})^T = (\mu_r^1 - \mu_r^0) \quad (2)$$

where  $(b_{r,0} \ b_{r,1} \ \dots \ b_{r,p-1})$  is composed of  $b_{r,i}$ ; when  $i = x$ ,  $b_{r,i} = 1$ ; when  $i = y$ ,  $b_{r,i} = -1$ ; and in other cases,  $b_{r,i} = 0$ . Then, for the  $q$  pairs of overlapped areas,  $q$  equations, such as in (2), can be listed

$$\begin{pmatrix} b_{0,0} & b_{0,1} & \dots & b_{0,p-1} \\ b_{1,0} & b_{1,1} & \dots & b_{1,p-1} \\ \dots & \dots & \dots & \dots \\ b_{q-1,0} & b_{q-1,1} & \dots & b_{q-1,p-1} \end{pmatrix} \begin{pmatrix} \mu_0 \\ \mu_1 \\ \dots \\ \mu_{p-1} \end{pmatrix} = \begin{pmatrix} \mu_0^1 - \mu_0^0 \\ \mu_1^1 - \mu_1^0 \\ \dots \\ \mu_{q-1}^1 - \mu_{q-1}^0 \end{pmatrix}. \quad (3)$$

Equation (3) can be written as  $A_B X_\mu = L_B$ .

*Step 2.2:* Construct the matrix equation set by a reference image.

Assuming that the difference of actual mean between the reference image and the ideal mean is small or almost zero, the  $s$ th image is a reference image, which could be described

$$(c_{s,0} \ c_{s,1} \ \dots \ c_{s,p-1})(\mu_0 \ \mu_1 \ \dots \ \mu_{p-1})^T = 0 \quad (4)$$

where  $(c_{s,0} \ c_{s,1} \ \dots \ c_{s,p-1})$  is composed of  $c_{s,j}$ ; when  $j = s$ ,  $c_{s,j} = 1$ ; and in other cases,  $c_{s,j} = 0$ . Suppose that  $t$  reference images are selected from the  $p$  images, and the equation sets are listed

$$\begin{pmatrix} c_{0,0} & c_{0,1} & \dots & c_{0,p-1} \\ c_{1,0} & c_{1,1} & \dots & c_{1,p-1} \\ \dots & \dots & \dots & \dots \\ c_{t-1,0} & c_{t-1,1} & \dots & c_{t-1,p-1} \end{pmatrix} \begin{pmatrix} \mu_0 \\ \mu_1 \\ \dots \\ \mu_{p-1} \end{pmatrix} = \begin{pmatrix} 0 \\ 0 \\ \dots \\ 0 \end{pmatrix}. \quad (5)$$

Equation (5) can be written as  $A_C X_\mu = L_C$ .

*Step 2.3:* Construct the error equation set.

Unite the matrix equation set by overlapped areas and matrix equation set by reference image, and get  $A X_\mu = L$ , where  $A = (A_B^T \ A_C^T)^T$  and  $L = (L_B^T \ L_C^T)^T$ .

*Step 2.4:* Construct the weight matrix.

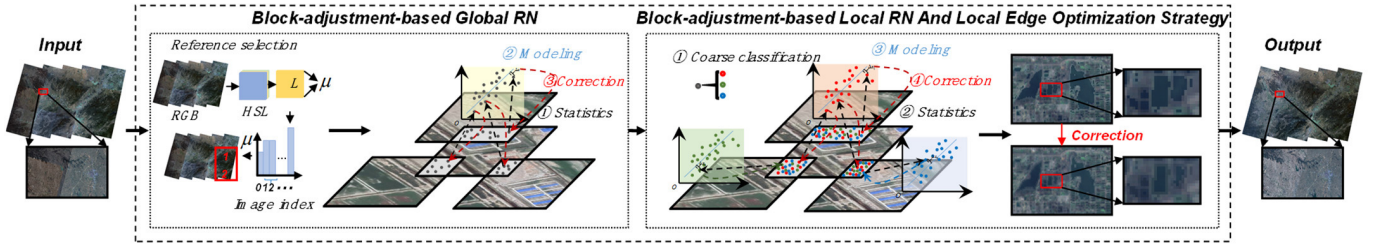


Fig. 1. Flowchart of the proposed method. The block-adjustment-based global RN module is the global model, which includes two core processes: the selection of the reference image and the construction of the block adjustment model. The block-adjustment-based local RN and local edge optimization strategy module contains two local models.

To determine the effect of each pair of overlapped areas, a weight matrix  $P$  is constructed

$$P = \begin{pmatrix} W & O \\ O & E \end{pmatrix} \quad (6)$$

$$w_i = n_i / \sum_{j=0}^{q-1} n_j \quad (7)$$

where  $O$  is a zero matrix,  $E$  is an identity matrix of order  $(t \times t)$ ,  $W$  is a diagonal matrix composed of  $w_{ii}$ ,  $i \in [0, q-1]$ , and  $n_i$  represents the number of pixels in the  $i$ th overlapped area.

*Step 2.5:* Solve the compensation parameters.

Use the least squares to solve the mean compensation parameters as follows:

$$X_\mu = (A^T P A)^{-1} A^T P L. \quad (8)$$

Similarly, standard deviation compensation parameters can be obtained according to Step 2

$$\begin{cases} X_\mu = (\mu_0 & \mu_1 & \dots & \mu_{p-1}) \\ X_\delta = (\delta_0 & \delta_1 & \dots & \delta_{p-1}) \end{cases} \quad (9)$$

where  $X_\mu$  and  $X_\delta$  represent the compensation parameters of the mean and standard deviation of  $p$  images, respectively.

*Step 3 (MM correction):* MM is employed to correct the target image. Supposing that the target image  $h$  intersects with the image  $g_0, g_1, \dots, g_{\text{num}-1}$  in the overlapped areas  $I_0, I_1, \dots, I_{\text{num}-1}$ ,  $\text{num}$  represents the number of images overlapped with the image  $h$ . Then, for the image adjacent to the target image, the ideal values of pixel standard deviation and mean of the overlapped area are

$$\begin{cases} \delta_{\text{ref}}^i = \delta_{I_i}^{g_i} + \delta_{g_i} \\ \mu_{\text{ref}}^i = \mu_{I_i}^{g_i} + \mu_{g_i} \end{cases} \quad (10)$$

where  $\delta_{\text{ref}}^i$  and  $\mu_{\text{ref}}^i$  represent the ideal standard deviation and mean of the image  $g_i$  in the overlapped area  $I_i$ , respectively,

$\delta_{g_i}$  and  $\mu_{g_i}$  represent the compensation parameters of standard deviation and mean of image  $g_i$ , respectively, and  $\delta_{I_i}^{g_i}$  and  $\mu_{I_i}^{g_i}$  represent the actual values of the standard deviation and mean of the image  $g_i$  in the overlapped area  $I_i$ , respectively.

For each overlapped area  $I_i$  of the target image  $h$ , the weight  $w_i$  is

$$w_i = n_i / \sum_{j=0}^{\text{num}-1} n_j \quad (11)$$

where  $n_i$  represents the number of pixels in the overlapped area. Therefore, for the target image  $h$ , the reference standard deviation  $\delta_{\text{ref}}$  and reference mean  $\mu_{\text{ref}}$  are

$$\begin{cases} \delta_{\text{ref}} = \sum_{i=0}^{\text{num}-1} (\delta_{\text{ref}}^i \times w_i) \\ \mu_{\text{ref}} = \sum_{i=0}^{\text{num}-1} (\mu_{\text{ref}}^i \times w_i). \end{cases} \quad (12)$$

The target standard deviation and target mean of the target image  $h$  are

$$\begin{cases} \delta_{\text{dst}} = \sum_{i=0}^{\text{num}-1} (\delta_{I_i}^h \times w_i) \\ \mu_{\text{dst}} = \sum_{i=0}^{\text{num}-1} (\mu_{I_i}^h \times w_i) \end{cases} \quad (13)$$

where  $\delta_{I_i}^h$  and  $\mu_{I_i}^h$  represent the actual values of the standard deviation and mean of the image  $h$  in the overlapped area  $I_i$ , respectively. Then, MM is applied to correct the target image  $h$ . For all target images, the correction is carried out according to Step 3.

### B. Block-Adjustment-Based Local RN and Local Edge Optimization Strategy

In order to solve the tone discontinuity of local features, a local RN method based on block adjustment is proposed. This method mainly includes four steps: image coarse classification, information statistics of overlapped area, block adjustment modeling, and MM correction. Our RN is applied to the digital number (DN) values of remote sensing images. DN values are converted first to normalized vegetation index (NDVI) for each image. Then, the images are roughly divided into four categories according to NDVI:  $-1 \leq \text{NDVI} < 0$ ,  $0 \leq \text{NDVI} < 0.33$ ,  $0.33 \leq \text{NDVI} < 0.66$ , and  $0.66 \leq \text{NDVI} \leq 1$ . Among them, the negative value of NDVI means that the ground cover is cloud, water, snow, and so on, and the nonnegative values are equally divided. Every category is separately corrected in a band-by-band way based on block adjustment as in Section II-A.

In order to further solve the artifacts of the local water edge, a local edge optimization strategy is proposed. This method essentially constructs a cumulative error allocation strategy around the water edge. As shown in Fig. 2, the red line represents the boundary between local water features and



Fig. 2. Local edge optimization.

nonwater features in the image. The local edge optimization strategy mainly includes two steps.

*Step 1 (Buffer Setting):*

Taking the red line as the boundary and taking the same size area on each side as a buffer, the buffer is divided into  $2n$  parts, numbered  $0, 1, \dots, 2n-1$ . The outermost areas  $0$  and  $2n-1$  on both sides are set as the reference for the inner area, and RN will be performed on the inner  $2n-2$  areas. The difference  $\mu_{\text{dif}}$  between means and the difference  $\delta_{\text{dif}}$  between standard deviations of area  $0$  and area  $2n-1$  are as follows:

$$\begin{cases} \mu_{\text{dif}} = \mu_{2n-1} - \mu_0 \\ \delta_{\text{dif}} = \delta_{2n-1} - \delta_0 \end{cases} \quad (14)$$

where  $\mu_i$  and  $\delta_i$  represent the pixel mean and standard deviation of area  $i$ , respectively. Then, the interval mean  $\mu_{\text{gap}}$  and interval standard deviation  $\delta_{\text{gap}}$  are

$$\begin{cases} \mu_{\text{gap}} = \mu_{\text{dif}}/(2n-2) \\ \delta_{\text{gap}} = \delta_{\text{dif}}/(2n-2). \end{cases} \quad (15)$$

*Step 2 (MM correction):*

For the inner  $2n-2$  target areas, the reference mean and standard deviation are solved as follows:

$$\begin{cases} \mu'_i = \mu_i + i \times \mu_{\text{gap}} \\ \delta'_i = \delta_i + i \times \delta_{\text{gap}} \end{cases} \quad (16)$$

where  $i$  represents the label of the inner area,  $i \in [1, 2n-2]$ ,  $\mu_i$  and  $\delta_i$  represent the mean and standard deviation of the inner area  $i$ , respectively, and  $\mu'_i$  and  $\delta'_i$  represent the reference mean and reference standard deviation of the inner area  $i$ , respectively. The RDs of the inner  $2n-2$  areas are corrected with MM.

Through such a global-to-local RN, we have completed the elimination of the RDs of MRS images.

### III. EXPERIMENTAL RESULTS AND ANALYSIS

We selected two data sets from Landsat-8 OLI. The four, three, and two bands are selected as experimental data. The first data set (15 images) covers Central China from 2016 to 2018, and the second data set (12 images) covers North China from 2017 to 2019.

In order to further evaluate the proposed method, the RN module of ENVI IDL Version 5.3 (histogram matching) and MM with the one-after-another pipeline were considered as the comparison methods. For the three methods, the reference image is the same. For convenience, the proposed method, ENVI method, and MM with the one-after-another pipeline are referred to as ‘‘BARN,’’ ‘‘ENVI,’’ and ‘‘MM,’’ respectively.

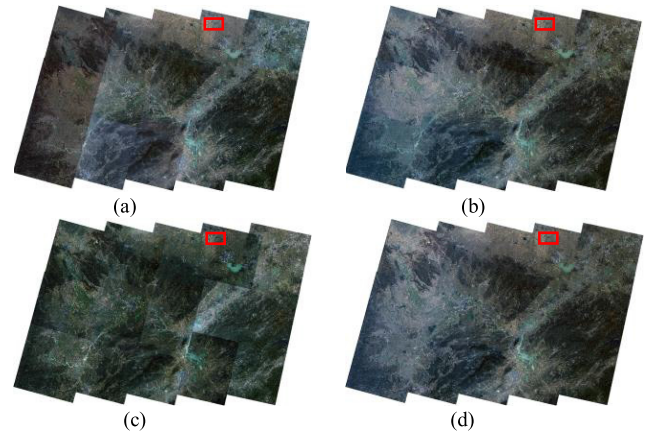


Fig. 3. Result comparisons of the first data set. (a) Original. (b) MM. (c) ENVI. (d) BARN.

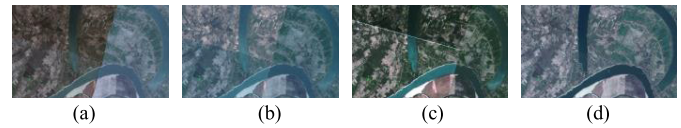


Fig. 4. Detailed comparisons of Fig. 3. (a) Original. (b) MM. (c) ENVI. (d) BARN.

#### A. Visual Assessments

There are obvious RDs between adjacent images in the two data sets. Fig. 3 shows the results of the first data set. It can be clearly seen that the results of the proposed method are visually seamless and consistent. The result of MM was enhanced, but there are obvious RDs between some adjacent images. This is because MM deeply depends on the transfer paths. The ENVI results are relatively poor. Fig. 4 shows the details in the red box shown in Fig. 3. It is obvious that the proposed method is superior to others. Fig. 5 shows the results of the second data set. The results of MM are good, but those of the proposed method are slightly better. Both BARN and MM are applicable to images with global RDs. The ENVI results are the worst. Fig. 6 shows the details in the red box shown in Fig. 5. In general, BARN can obtain MRS images with a balanced and appealing visual effect, which achieves the best results compared with MM and ENVI.

#### B. Quantitative Analysis

To further evaluate the proposed method objectively, two metrics were used to evaluate the RDs between adjacent images, including the absolute differences of the mean and standard deviation of the overlapped areas [15], as follows:

$$\begin{cases} D_\mu = \sum_{i=0}^q |\Delta M_i|/q \\ D_\delta = \sum_{i=0}^q |\Delta S_i|/q \end{cases} \quad (17)$$

where low values indicated that small RDs exist between MRS images.  $D_\mu$  is the absolute difference of the mean of the overlapped areas of the images,  $D_\delta$  is the absolute difference of the standard deviation of the overlapped areas of the images,  $q$  indicates that there are  $q$  overlapping pairs, and  $\Delta M_i$  and  $\Delta S_i$  represent the difference of the mean and the standard

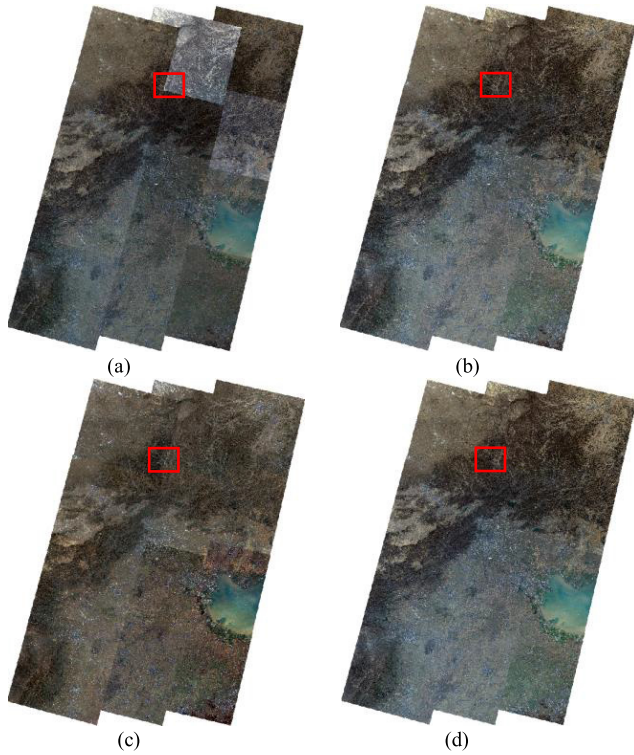


Fig. 5. Result comparisons of the second data set. (a) Original. (b) MM. (c) ENVI. (d) BARN.

TABLE I

ABSOLUTE DIFFERENCE OF MEAN AND STANDARD DEVIATION BETWEEN OVERLAPPED AREAS WITH DIFFERENT METHODS

Dataset	Metrics	Original	MM	ENVI	BARN(ours)
First	$D_\mu$	447.7471	428.9449	-	<b>378.5443</b>
	$D_\delta$	295.9119	278.0091	-	<b>244.2963</b>
Second	$D_\mu$	456.6329	311.7452	-	<b>305.6291</b>
	$D_\delta$	291.5473	145.5421	-	<b>140.0995</b>

deviation of the  $i$ th overlapping area, respectively. Table I shows the absolute differences of the mean and standard deviation for the same position between the original images and the normalized images; they indicate the differences in the statistical distribution.

In Table I, the bold numbers are the minimum value of each row, indicating that the results of the corresponding method have the smallest RDs. In addition, since ENVI cannot give results that are not stitched in the intermediate process, the metrics cannot be calculated. It can be seen that the RDs of the original images are large, which has been improved by different methods. The proposed method has the best results. It can be seen from the first data set that the values of the proposed method and MM have greatly decreased, indicating that they perform well. The proposed method achieved the best results. For the second data set, the values of the proposed method and MM are relatively close, indicating that the two methods have a good effect of eliminating the overall RDs. The values of the proposed method are slightly lower, indicating that the results of the proposed method are better. The quantitative evaluation result is consistent with the visual evaluation.

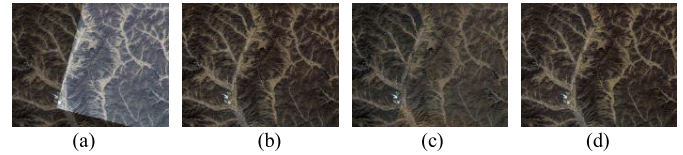


Fig. 6. Detailed comparisons of Fig. 5. (a) Original. (b) MM. (c) ENVI. (d) BARN.

#### IV. CONCLUSION

In this letter, we proposed a block adjustment-based RN method of MRS images by considering global and local RDs. Under the framework of the combined model, BARN solves the problem of error accumulation and adaptive allocation of cumulative errors caused by the transfer paths in the classical one-after-another pipeline. The experiment confirms that the proposed method can obtain the visual consistency of MRS images, which is promising for the large-scale application of remote sensing images. In the future, we will further improve efficiency and carry out more tests.

#### REFERENCES

- [1] X. Li, N. Hui, H. Shen, Y. Fu, and L. Zhang, "A robust mosaicking procedure for high spatial resolution remote sensing images," *ISPRS J. Photogramm. Remote Sens.*, vol. 109, pp. 108–125, Nov. 2015.
- [2] L. Yu, Y. Zhang, M. Sun, X. Zhou, and C. Liu, "An auto-adapting global-to-local color balancing method for optical imagery mosaic," *ISPRS J. Photogramm. Remote Sens.*, vol. 132, pp. 1–19, Oct. 2017.
- [3] X. Li, R. Feng, X. Guan, H. Shen, and L. Zhang, "Remote sensing image mosaicking: Achievements and challenges," *IEEE Geosci. Remote Sens. Mag.*, vol. 7, no. 4, pp. 8–22, Dec. 2019.
- [4] B. Arbelot, R. Vergne, T. Hurtut, and J. Thollot, "Local texture-based color transfer and colorization," *Comput. Graph.*, vol. 62, pp. 15–27, Feb. 2017.
- [5] M. He, J. Liao, D. Chen, L. Yuan, and P. V. Sander, "Progressive color transfer with dense semantic correspondences," *ACM Trans. Graph.*, vol. 38, no. 2, pp. 1–18, Apr. 2019.
- [6] Z. Su, K. Zeng, L. Liu, B. Li, and X. Luo, "Corruptive artifacts suppression for example-based color transfer," *IEEE Trans. Multimedia*, vol. 16, no. 4, pp. 988–999, Jun. 2014.
- [7] C. Cariou and K. Chehdi, "Fully automated mosaicking of pushbroom aerial imagery," in *Proc. IEEE Int. Conf. Acoust., Speech Signal Process.*, Mar. 2008, pp. 1105–1108.
- [8] X. Han, H. Cao, Z. Yuan, H. Zhao, and L. Yan, "An approach of color image mosaicking based on color vision characteristics," in *Proc. 3rd Int. Conf. Genetic Evol. Comput.*, Oct. 2009, pp. 343–346.
- [9] M. Sun and J. Q. Zhang, "Dodging research for digital aerial images," *Int. Arch. Photogramm. Remote Sens. Spat. Inf. Sci.*, vol. 37, pp. 349–353, Jan. 2008.
- [10] R. Xie, M. Xia, J. Yao, and L. Li, "Guided color consistency optimization for image mosaicking," *ISPRS J. Photogramm. Remote Sens.*, vol. 135, pp. 43–59, Jan. 2018.
- [11] M. Xia, J. Yao, and Z. Gao, "A closed-form solution for multi-view color correction with gradient preservation," *ISPRS J. Photogramm. Remote Sens.*, vol. 157, pp. 188–200, Nov. 2019.
- [12] L. Li, Y. Li, M. Xia, Y. Li, J. Yao, and B. Wang, "Grid model-based global color correction for multiple image mosaicking," *IEEE Geosci. Remote Sens. Lett.*, early access, Jul. 27, 2020, doi: [10.1109/LGRS.2020.3009671](https://doi.org/10.1109/LGRS.2020.3009671).
- [13] J. Li, Q. Hu, and M. Ai, "Optimal illumination and color consistency for optical remote-sensing image mosaicking," *IEEE Geosci. Remote Sens. Lett.*, vol. 14, no. 11, pp. 1943–1947, Nov. 2017.
- [14] J. Pan, M. Wang, D. Li, and J. Li, "A network-based radiometric equalization approach for digital aerial orthoimages," *IEEE Geosci. Remote Sens. Lett.*, vol. 7, no. 2, pp. 401–405, Apr. 2010.
- [15] L. Zhang, C. Wu, and B. Du, "Automatic radiometric normalization for multitemporal remote sensing imagery with iterative slow feature analysis," *IEEE Trans. Geosci. Remote Sens.*, vol. 52, no. 10, pp. 6141–6155, Oct. 2014.